Optical properties and damage analysis of GaAs single crystals partly amorphized by ion implantation

M. Erman, J. B. Theeten, and P. ChambonS. M. KelsoD. E. Aspnes

Citation: **56**, 2664 (1984); doi: 10.1063/1.333785
View online: http://dx.doi.org/10.1063/1.333785
View Table of Contents: http://aip.scitation.org/toc/jap/56/10
Published by the American Institute of Physics

Optical properties and damage analysis of GaAs single crystals partly amorphized by ion implantation

M. Erman, J. B. Theeten, and P. Chambon
Laboratoires d'Electronique et de Physique Appliquée, 3, avenue Descartes-94450 Limeil-Brévannes, France

S. M. Kelso
Xerox Palo Alto Research Center, Palo Alto, California 94304

D. E. Aspnes
Bell Communications Research, Murray Hill, New Jersey 07974

(Received 6 April 1984; accepted for publication 8 June 1984)

Dielectric functions of partly amorphized GaAs layers produced by deep ion implantation of different doses of 270-keV As^+ ions in crystalline (*c*-) GaAs have been measured from 1.5 to 6.0 eV by spectroscopic ellipsometry. We show that these dielectric functions cannot be described as physical mixtures of amorphous (*a*-) and *c*-GaAs, as such models exhibit strong deviations with respect to the data near 3 eV. We determine representations of these dielectric functions as finite sums of harmonic oscillators, which allows us to describe these spectra as analytic functions of a single parameter related to the amount of damage. In this harmonic oscillator approximation (HOA), we show that damage profiles of ion-implanted material can be nondestructively determined from ellipsometric spectra in terms of multilayer models. In a representative case, good agreement is found between damage profiles determined nondestructively in the HOA and destructively by chemical etching.

I. INTRODUCTION

It is well known that medium- or heavy-ion implantation in crystalline semiconductors locally destroys the lattice perfection and leaves a trail of defects in an otherwise perfect crystal. By performing ion implantations at various fluences, it is possible to obtain materials with properties continuously variable from crystalline to amorphous. For instance, the characteristic structures of the dielectric function of crystalline GaAs slowly vanish as the dose of implantation increases.[1] A physical or analytical model describing the dielectric response of the semiconductor in intermediate stages between that of the perfect crystal and the totally amorphous structure would be important, because then the implantation damage could be nondestructively profiled by spectroscopic ellipsometry, as discussed in Ref. 2. A usual way of describing the dielectric response of these intermediate stages is to assume that the material is a physical mixture of crystalline and amorphous GaAs and to use the effective medium approximation (EMA)[3] or a similar mean-field theory to calculate the resulting dielectric function. We show in this paper that the EMA is a rather poor aproximation for intermediate-stage materials, particularly near 3 eV, where the E_1 and $E_1+\Delta_1$ structures disappear more rapidly than the E_0' and E_2 structures near 5 eV. As we will show, this behavior cannot be described by means of any physical mixture model.

To allow us to achieve our objective of nondestructive damage analysis, we use a purely phenomenological approach where the dielectric function ϵ is represented analytically from 1.5 to 6.0 eV as a superposition of harmonic oscillators. Similar methods have been used previously to represent reflectivity spectra or dielectric functions calculated from measured reflectivity spectra for Si and Ge.[4–6] In this paper, we use the real and imaginary parts of the dielectric function measured directly by spectroscopic ellipsometry, without needing assumptions about experimentally inaccessible spectral regions.

In our harmonic oscillator approximation (HOA) we use a set of seven harmonic oscillators. The amplitudes, energies, and broadening parameters are chosen to minimize the mean-square deviation between the measured and calculated ϵ spectra. Representing these parameters in turn as functions of a single additional parameter, the implantation fluence, we obtain a purely analytical one-parameter description of ϵ, accurate to within 1%, which can be continuously varied from crystalline to amorphous material. The HOA is used to nondestructively determine the damage profile of a specific sample of ion-implanted GaAs, and the results are compared to those of destructive measurements using chemical etching. Good agreement is found.

II. DIELECTRIC FUNCTION OF PARTIALLY AMORPHIZED GaAs

A. Experiment

Partly amorphized (100) GaAs layers were obtained by 7° off-axis implantation of *n*-type ($N_D \sim 2\times10^{17}\,cm^{-3}$) GaAs single crystals with 270-keV As^+ ions at various fluences. The penetration depth of these ions, 120 nm, is larger than the penetration of the light at energies greater than 2 eV. Therefore, from the standpoint of optical measurements, these implanted layers can be considered equivalent to infinitely thick bulk material. Dielectric function spectra from 1.5 to 6.0 eV were obtained for these samples using instrumentation[7] [rotating analyzer ellipsometer (RAE)] and preparation[8] techniques described elsewhere. The measured dielectric functions for various fluences are plotted in Figs. 1(a) and 1(b). This figure shows clearly how

 0021-8979/84/222664-08$02.40

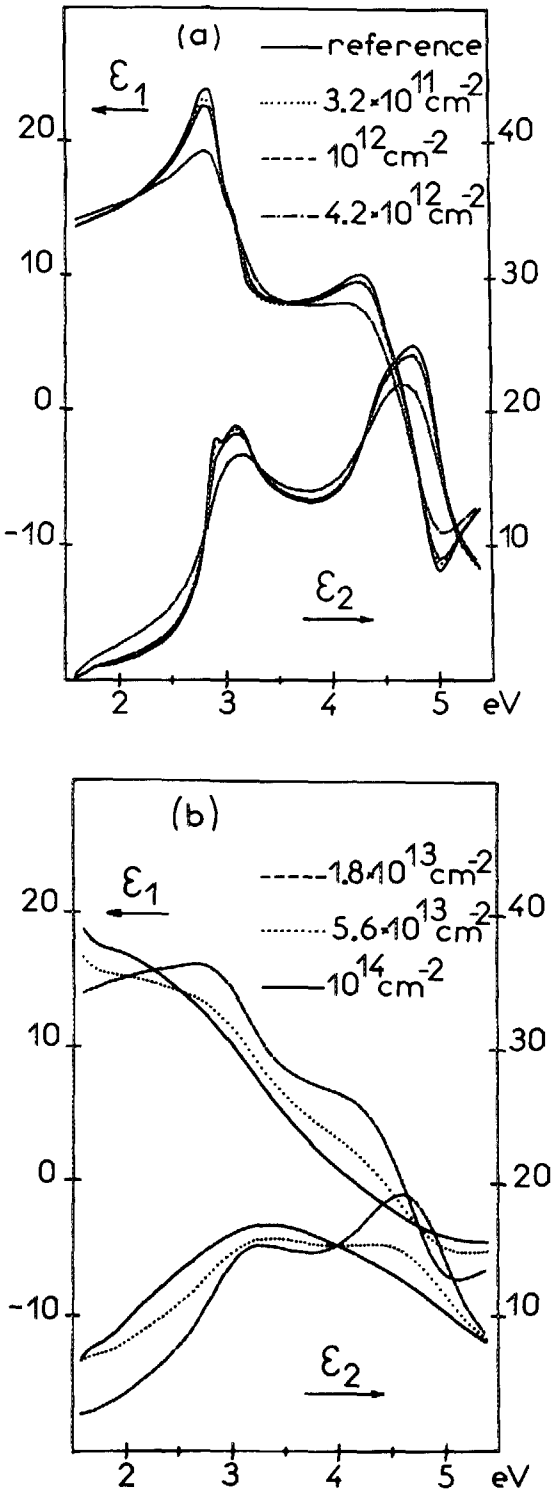

FIG. 1. Dielectric function of crystalline GaAs and GaAs implanted with 270-keV As^+ at various fluences.

the characteristic structures in ϵ for crystalline GaAs (*c*-GaAs) vanish as the fluence is increased. At low energies (1.6 eV $< E <$ 2 eV) and high fluences (1×10^{14} cm^{-2}), interference oscillations due to the finite thickness of the damaged layer can be seen.

B. Physical mixing models: Effective medium theories

The partially disordered material obtained after moderate ion implantation can be described as a heterogeneous medium composed of microscopic regions with local order ranging from perfectly crystalline to fully amorphous. One approach is to assume that the material can be described everywhere as being *either* crystalline *or* amorphous with the dielectric response being given by the appropriate limiting material of infinite extent. (This supposes in addition no changes in structure, i.e., the fourfold coordination of each Ga and As atom.) If the regions are also small compared to the wavelength of light, then only average properties can be measured and the dielectric response can be calculated by effective medium theory.

If the exact microstructure were known, one could, in principle, first solve the microscopic (local field) problem exactly, and then average the microscopic solutions to obtain the corresponding macroscopic observables.[9] It can be shown that even if no information is available about either

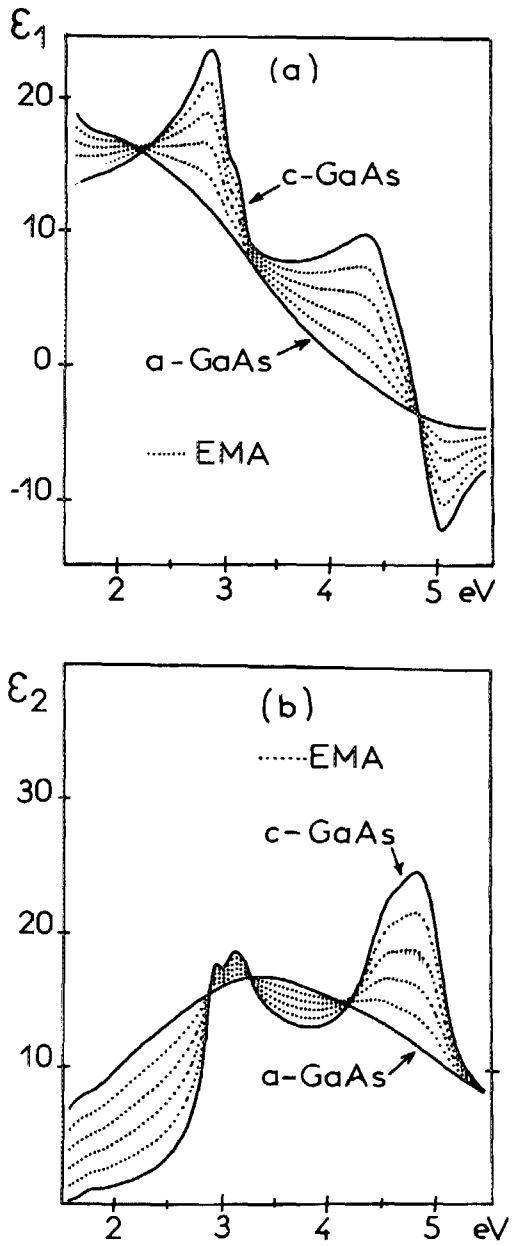

FIG. 2. Dielectric functions calculated by the EMA for several physical mixtures of *c*-GaAs and *a*-GaAs. (a) Real part ϵ_1. (b) Imaginary part ϵ_2.

composition or microstructure, the possible values of ϵ must still lie between two well-defined limits: the so-called Wiener bounds.[10] The two extreme cases correspond to no screening and maximum screening. If ϵ_A and ϵ_B are the dielectric functions of the materials A and B, respectively, and f_A and f_B are the relative volume fractions, then the Wiener limits are given by

$$\langle\epsilon\rangle = f_A\epsilon_A + f_B\epsilon_B \quad \text{for no screening} \tag{1}$$

and

$$\langle\epsilon\rangle = (f_A/\epsilon_A + f_B/\epsilon_B)^{-1} \quad \text{for maximum screening.} \tag{2}$$

The region enclosed by the two limits represents the allowed values of ϵ for any effective medium theory. More commonly, a spherical microstructure is assumed, in which case ϵ is given by

$$\frac{\langle\epsilon\rangle - \epsilon_H}{\langle\epsilon\rangle + 2\epsilon_H} = f_A \frac{\epsilon_A - \epsilon_H}{\epsilon_A + 2\epsilon_H} + f_B \frac{\epsilon_B - \epsilon_H}{\epsilon_B + 2\epsilon_H}, \tag{3}$$

where ϵ_H is the dielectric function of the "host" medium.[11] Thus if A or B is the "host" material, the $\epsilon_H = \epsilon_A$ or $\epsilon_H = \epsilon_B$ and the Maxwell–Garnett expressions are obtained. These expressions are useful for deriving more restrictive limit theorems,[12–14] but we shall not need them here. A more useful effective medium theory (EMT) is the self-consistent choice $\epsilon_H = \epsilon$, in which case the Bruggeman effective medium approximation (EMA)[3] is obtained. Figures 2(a) and 2(b) show how ϵ should be expected to evolve with fluence in the EMA.

Figure 3 illustrates the range of the EMA and two Maxwell–Garnett approximations within the Wiener limits for the specific case $\epsilon_A = 3 + i2$ and $\epsilon_B = -2 + i4$. It should be noted that for isotropic mixtures ϵ must lie between the

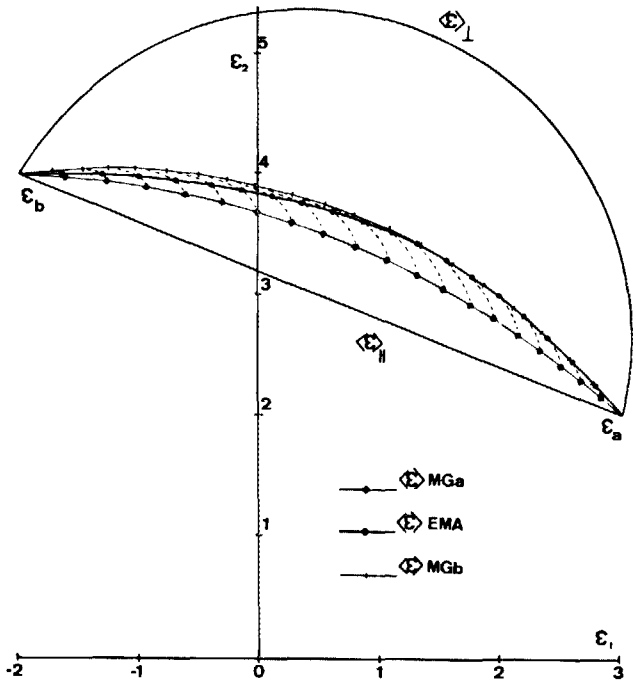

FIG. 3. Allowed values of the dielectric functions of a physical mixture $A + B$, with $\epsilon_A = 3 + i2$ and $\epsilon_B = -2 + i4$. The allowed domain is limited by the Wiener bounds $\langle\epsilon\rangle_\parallel$ and $\langle\epsilon\rangle_\perp$. We have also represented the curves obtained with the Maxwell–Garnett approximations MGa ($\epsilon_H = \epsilon_A$) and MGb ($\epsilon_H = \epsilon_B$) and the Bruggeman EMA.

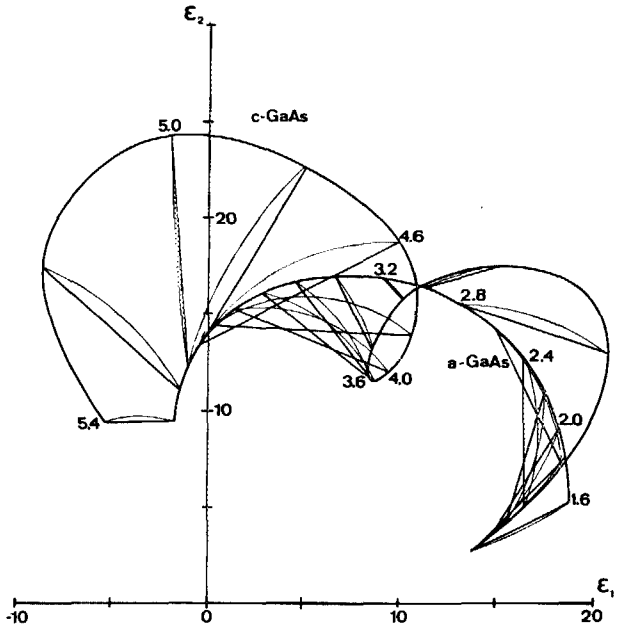

FIG. 4. Allowed values (Wiener bounds) of the dielectric function corresponding to a physical mixture of c-GaAs and a-GaAs. The domains are plotted for various energies from 1.6 to 5.4 eV in steps of 200 meV.

two Maxwell–Garnett curves.[12–14] We have also calculated the Wiener bounds at different energies for a mixture of a-GaAs and c-GaAs. The results are plotted in Fig. 4. In order to make this figure clearer, we do not show the curves corresponding to the Maxwell–Garnett and Bruggeman models. From Fig. 3 it can be appreciated that the allowed values for ϵ for isotropic samples will lie in domains much smaller than those in Fig. 4.

The measured dielectric functions of some partly amorphized GaAs samples are compared to the Wiener limits of the physical mixing model for five energies in Fig. 5. It is clear that the Wiener bounds themselves, to say nothing of the more restrictive limits applicable to isotropic samples, are strongly violated below 4 eV. This is especially true near 3 eV, i.e., near the E_1 and $E_1 + \Delta_1$ structures. At this energy

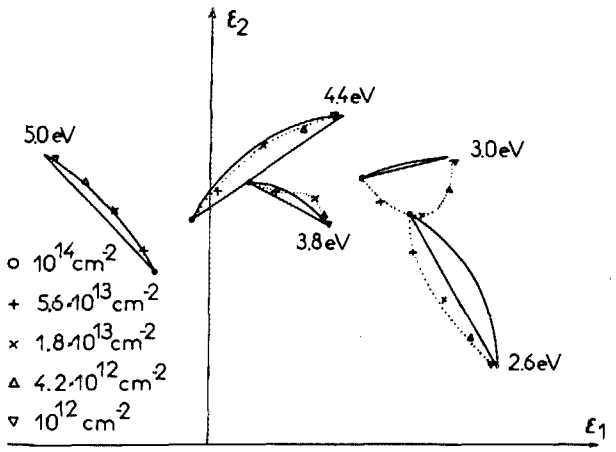

FIG. 5. Comparison of the allowed domains of $\langle\epsilon\rangle$ (curves) and the experimental data (symbols) corresponding to the crystalline-to-amorphous transition at 2.6, 3.0, 3.8, 4.4, and 5.0 eV.

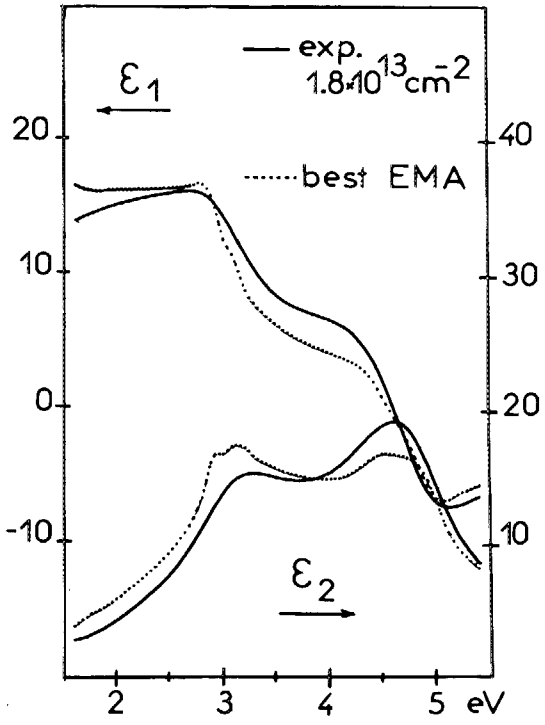

FIG. 6. Comparison of the dielectric function measured on the sample implanted at 1.8×10^{13} cm^{-2} and the "best" (i.e., corresponding to the lowest mean-square deviation) dielectric function in the EMA.

the experimental data lie completely outside the Wiener bounds. This demonstrates that no physical mixture model can describe ion-implanted material.

Another way to illustrate the feature of physical mixture models in this case is shown in Fig. 6. Here, we give the ϵ spectra for a sample implanted to 1.8×10^{13} cm^{-2} and calculate the best fit within the EMA. Note that it is impossible to fit the whole spectral region because the structures at 3 eV vanish at lower fluences than do those at 5 eV. As already reported,[1] this is due to different characteristic ranges of the excitations associated with the optical transitions. It was found in Ref. 1 that the projected areas obtained for the E_1, $E_1+\Delta_1$, E_0', and E_2 excitonic resonances are (10 nm)^2, (9 nm)^2, (8.2 nm)^2, and (6.3 nm)^2, respectively. Consequently, the assumption that moderately-implanted material can be described as a two-phase mixture with the dimensions of each domain being large enough for the dielectric function of bulk material to be acceptable cannot be true. The polarizability of a given region is itself a function of the size of the region, and a proper description of ϵ must take this explicitly into account.

C. Harmonic oscillator approximation

A first principles description of the dielectric response of partially amorphized material would be a difficult challenge. For the purposes of materials analysis, we shall deal in a phenomenological manner with the inability of effective medium theories to describe implanted material. We shall consider each fluence to produce a new material and use its measured spectrum to define ϵ. We next use sets of harmonic oscillators to fit the measured dielectric functions. This spectral representation provides us with an analytic description of ϵ as a function of fluence, and by interpolating the coefficients we can obtain a representation of ϵ for any fluence. By using harmonic oscillators as a basis, the causality, linearity, reality, and Kramers–Kronig requirements, compulsory properties of ϵ, are satisifed automatically.

The dielectric response of a single harmonic oscillator is given by the following expression:

$$\epsilon(E)=1+\left(\frac{\hbar\omega_p}{2E_0}\right)^2\left(\frac{1}{E+E_0+i\Gamma}-\frac{1}{E-E_0+i\Gamma}\right), \quad (4)$$

where E_0 is the energy of the harmonic oscillator, Γ is the broadening parameter, and ω_p is the plasmon frequency. The lineshapes of the real and imaginary parts of $\epsilon(E)$ are shown in Fig. 7. As already noted, ϵ_1 and ϵ_2 are Kramers–Kronig transforms of each other.

The dielectric response of a real solid can be expressed as a superposition of such oscillators (the spectral representation).[15] For a perfect semiconductor crystal, ϵ is given by

$$\epsilon(E,\Gamma)=1+\frac{\hbar^2e^2}{\pi^2m^2E^2}\int_{\mathrm{BZ}}d^3k\,|\hat{e}\,P_{cv}(k)|^2 \times\left(\frac{1}{E+E_{cv}(k)+i\Gamma}-\frac{1}{E-E_{cv}(k)+i\Gamma}\right), \quad (5)$$

where $P_{cv}(k)$ is the momentum matrix element $\langle ck\,|p|vk\rangle$, c, v denote conduction and valence bands, $E_{cv}(k)=E_c(k)-E_v(k)$ is the interband energy, Γ is the phenomenological broadening parameter, and the integral is over the Brillouin zone.

However, this exact expression is too complicated to be useful for perfect crystals and, as written, does not apply to implanted material because momentum is not a good quantum number. We use the fact that the separate oscillators can be grouped by critical point to reduce the total number needed in the expression. This allows us also to separate the effects of fluence in different regions of the spectrum, since critical points broaden and weaken differently as the fluence destroys the momentum conservation upon which Eq. (5) is based. We have found that a minimum of seven oscillators are needed in this spectral region to fit the dielectric function of GaAs. Four correspond to the major optical transitions E_1, $E_1+\Delta_1$, E_0', and E_2. Two more are needed to describe general transitions between $E_1+\Delta_1$ and E_0' that are unre-

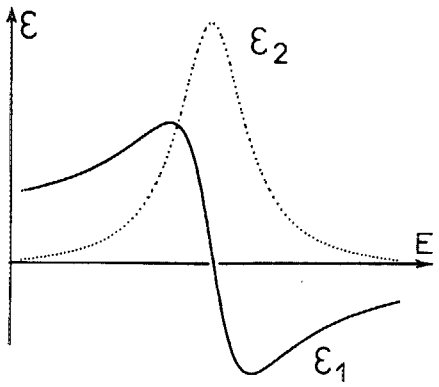

FIG. 7. Dielectric function of a single harmonic oscillator.

lated to any specific critical point, and one is needed with an energy greater than 5.5 eV to simulate the contribution of all optical transitions beyond our 1.5–5 eV energy range. The dielectric function can be then written in the following form:

$$\epsilon(E) = 1 + \sum_{k=1}^{7} A_k \left(\frac{1}{E + E_k + i\Gamma_k} - \frac{1}{E - E_k + i\Gamma_k} \right). \quad (6)$$

For c-GaAs, all 21 parameters, the energies E_k, broadening parameters Γ_k, and amplitudes A_k were determined by linear regression.[2] The convergence is good because the oscillators are only weakly correlated. The result of such a fitting using HOA is illustrated in Fig. 8. The residual for this fit is less than 1%, which is satisfactory since the absolute reproducibility in the measurement of dielectric functions is of the same order of magnitude.[16] We note that the HOA is only valid for photon energies larger than the fundamental absorption gap, because we have not included oscillators to represent the E_0 and $E_0 + \Delta_0$ transitions.

The remaining ϵ spectra of the implanted samples were fitted in a similar way using the same set of seven harmonic oscillators, except that the Γ_k and A_k were considered as adjustable parameters. The energies of the oscillators were taken to be the same as those obtained for c-GaAs. All values of Γ_k and A_k were then fitted with third-degree polynomials as a function of the fluence. The fluence 10^{14} ions/cm^2 was considered to correspond to a completely amorphous layer. The dielectric function of a partially amorphized GaAs sample is then given by Eq. (6),

with

$$\Gamma_k = \Gamma_k^0 + a_k x + b_k x^2 + c_k x^3 \quad (7)$$

and

$$A_k = A_k^0 + d_k x + e_k x^2 + f_k x^3, \quad (8)$$

TABLE I. Values of different constants involved in 7 HOA of the dielectric function of GaAs. For $x = 0$: crystalline GaAs. For $x = 1$: amorphous GaAs. Notice that A_6 can be negative; in this case, A_6 is set to zero.

	Energies
$i =$	E_i(eV)
1	2.9207
2	3.1267
3	3.5036
4	4.050
5	4.479
6	4.821
7	6.5595

Broadening parameter $\Gamma_i = \Gamma_i^0 + a_i x + b_i x^2 + c_i x^3$

$i =$	Γ_i^0	a_i	b_i	c_i
1	0.1249	+ 4.9905	− 7.2742	+ 3.0502
2	0.2160	+ 2.2396	− 2.2026	+ 0.9267
3	0.4114	+ 1.8653	− 0.2223	− 0.5712
4	0.4015	− 0.3315	+ 5.2172	− 3.7823
5	0.2693	+ 0.5805	+ 0.1482	− 0.1537
6	0.2918	+ 1.5980	− 6.4559	+ 7.1830
7	0.5828	+ 4.6604	− 7.5114	+ 3.8044

Amplitudes $A_i = A_i^0 + d_i n + e_i x^2 + f_i x^3$

$i =$	A_i^0	d_i	e_i	f_i
1	0.8688	+ 9.5850	− 15.175	+ 7.9389
2	2.3366	+ 5.0036	+ 0.0658	− 1.4494
3	3.2010	+ 1.7342	+ 11.185	+ 8.9020
4	2.1293	− 2.6888	+ 12.985	− 7.7394
5	2.6305	− 1.1120	+ 4.9966	− 3.8494
6	5.3206	− 16.373	+ 50.264	− 62.414
7	6.0531	+ 5.2147	− 19.307	+ 10.704

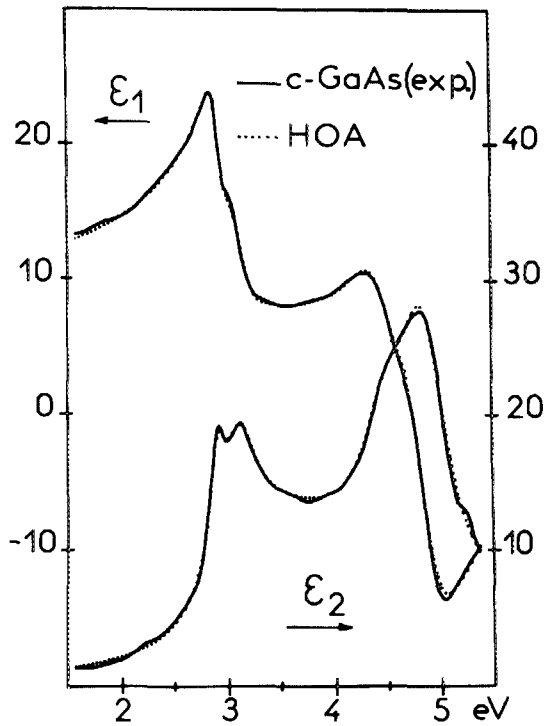

FIG. 8. Approximation to the dielectric function of c-GaAs using seven harmonic oscillators.

where x is the fluence normalized to 10^{14} cm^{-2}, i.e., x = fluence/(10^{14} cm^{-2}). Numerical values of the constants involved in this model are given in Table I.

We have compared the best approximations calculated in the EMA and HOA to the experimental curves. The mean square deviations were calculated for tan (ψ) and cos (Δ) rather ϵ_1 and ϵ_2, because these residuals can be directly compared with those obtained with the multilayer analysis of the next section. The results are plotted in Fig. 9. It is clear that

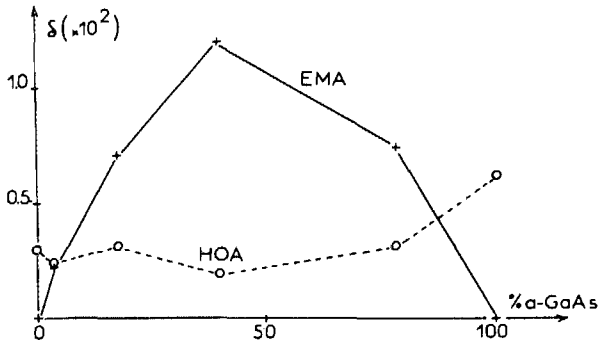

FIG. 9. Comparison of the experimental dielectric functions with the EMA (full line) and the HOA (dotted line) calculations. The error function is calculated on tan (ψ) and cos (Δ) curves for an angle of incidence of 66°.

the HOA is a much better approximation than the EMA for ion implanted layers. The error function is about 3×10^{-3}, which is small enough to make a multilayer analysis feasible for shallow implanted samples.

III. DAMAGE DEPTH PROFILING

In order to demonstrate the adequacy of the HOA, we have compared the damage profiles determined nondestructively from ellipsometric spectra with those obtained in a destructive way by etching the implanted wafers and measuring the global dielectric functions at each step.

For this comparison, we work with GaAs single crystals implanted to 2×10^{14} cm^{-2} of 10-keV Be^+. The mean projected range of the implanted atoms R_p is about 200 Å. It is obvious that the implanted sample cannot be considered as optically homogeneous in the 1.6–5.4 eV region. We measured the damage depth profile both by analyzing ellipsometric spectra and by chemical etching. The rotating polarizer ellipsometer (RPE) described elsewhere[17] was used for these measurements. The RPE and RAE ellipsometers have been compared earlier[18] and have been found to have similar accuracies.

A. chemical etching procedure

A 20/1/1 solution of $H_2SO_4/H_2O_2/H_2O$ was used as the etchant. The sample was rotated and one drop of the etchant was put on the surface of the wafer. The etching process was stopped by neutralizing the solution after a very short time (less than 1 sec). An automatic etching system was designed to obtain reproducible results by controlling etching and rinsing cycles, temperature, and rotation speed of the sample. In our system, one drop etched approximately 10 nm of *c*-GaAs. The cumulative microscopic roughness resulting from this etching process was less than two monolayers thick as measured by ellipsometry.

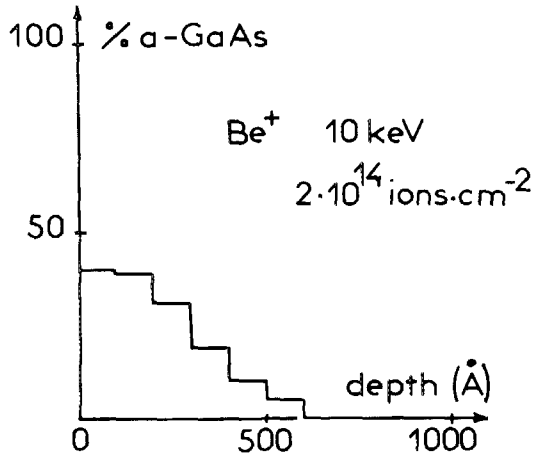

FIG. 10. Damage depth profile of GaAs implanted with 10-keV Be^+ at a fluence of 2×10^{14} cm^{-2} measured with chemical etching.

The damage depth profile was obtained by removing 100 nm in 10-nm steps. Ellipsometric spectra were measured at each stage. In order to obtain a parameter correlated with the amount of damage near the surface, we calculated the corresponding percentage of *a*-GaAs from the spectral region near 5 eV, where the penetration depth of the light is near 5 nm. Figure 10 shows the measured profile. The decrease of the damage with depth is clearly seen. From the surface to R_p (20 nm) the amount of damage seems to be relatively constant, but the resolution is not very good. Many other criteria could be used to characterize the amorphicity of implanted material. However, the resulting damage profiles have similar lineshapes.

TABLE II. Multilayer analysis of GaAs implanted with 10-keV Be^+ at a fluence of 2×10^{14} cm^{-2}.

3 parameters (+ oxide layer 12 Å thick)						
		GaAs 200 Å	GaAs 200 Å	Substrate	$10^3\,\delta$	
HOA	x	9.35	3.49	0.15	7.09	
	%*a*-GaAs	27.2	15.2	1.0		
EMA	%*a*-GaAs	29.7	27.5	4.25	21.2	
4 parameter (+ oxide layer 12 Å thick)						
		GaAs 50 Å	GaAs 200 Å	GaAs 200 Å	Substrate	$10^3\,\delta$
HOA	x	12.71	7.71	3.03	0.19	6.62
	%*a*-GaAs	32.3	24.1	13.6	1.0	
EMA	%*a*-GaAs	34.9	22.6	12.6	− 15.8	20.4
5 parameters (+ oxide layer 12 Å thick)						
		GaAs 20 Å	GaAs 50 Å	GaAs 200 Å	GaAs 200 Å	Substrate	$10^3\,\delta$
HOA	x	25.67	8.88	8.03	3.02	0.19	6.17
	%*a*-GaAs	45.5	25.9	25.0	13.3	1.0	
EMA	%*a*-GaAs	72.5	7.3	26.9	13.2	− 7.3	19.6

B. Multilayer analysis using EMA and HOA

The data obtained for the as-implanted sample were also analyzed (nondestructively) using multilayer analysis. Mathematical problems such as convergence and noise limitations have been discussed in Ref. 2. Several models with various numbers of parameters (i.e., layers) have been tested. Each model included a surface overlayer of oxide. Both the EMA and HOA were used to describe the damaged layers. The results are summarized in Table II. For the HOA we have indicated the normalized fluence x, as previously defined, and the corresponding percentage of a-GaAs. The function % (a-GaAs) $= f(x)$ is calculated for each x as being the best EMA fit to the dielectric function given by the HOA. Table II shows that for both models the error function decreases as the number of variable parameters increases. But we also notice that the error function is three times larger when the EMA is used instead of the HOA. A much better fit is obtained with the HOA as seen in Fig. 11 where we have compared the experimental curve with the two theoretical curves calculated for the last model (oxide layer/4 layers of GaAs/GaAs substrate). The final error function obtained with the HOA is of the same order of magnitude as the accuracy of the HOA model (Fig. 9). The resulting profile obtained with the HOA is plotted in Fig. 12. Except for the first 20-Å layer, this profile has the same line shape as the profile measured by chemical etching. The first layer is beyond the sensitivity of our etching method. Optically, this first layer appears to be absorbing, as already noticed.[2] This layer can simulate the changes induced by ion implantation at the interface between the oxide and the substrate. Because the dielectric function of a-GaAs is similar to the dielectric function of a-As, not included in our model, the changes at the interface could also be due to the reduction of the oxide, according to the following solid-state reaction[19]:

$$As_2O_3 + 2GaAs \rightarrow Ga_2O_3 + 4As.$$

The profile calculated by the EMA exhibits the same increase of the a-GaAs concentration near the surface. But this profile differs from the one calculated by the HOA, both by a dip in the profile corresponding to the second layer (5 nm thick) and by an unphysical result of a negative fraction of a-GaAs in the substrate. We believe that these are artifacts, due to the fact that the EMA does not accurately describe the optical properties of partially amorphized GaAs.

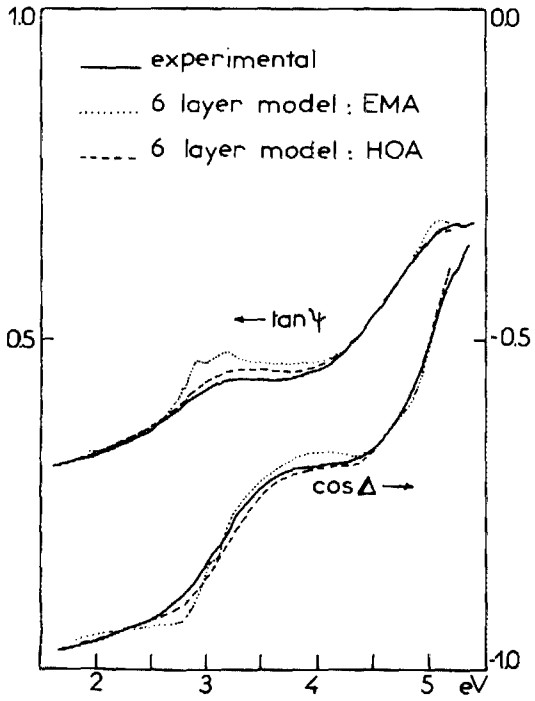

FIG. 11. Theoretical (EMA and HOA) and experimental ellipsometric curves for the sample of Fig. 10. The sample of incidence is 66°.

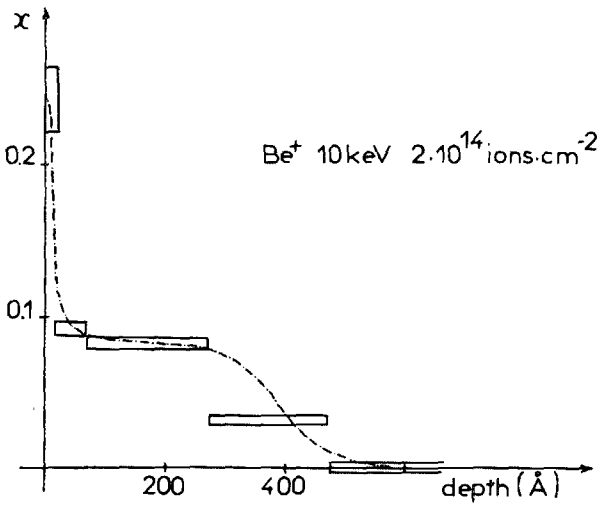

FIG. 12. Damage depth profile as calculated using the HOA and a five-parameter multilayer model (oxide/4 layers GaAs/GaAs substrate).

CONCLUSION

We have demonstrated that the dielectric fuction of a semiconductor (GaAs) can be represented accurately by an analytical expression based on a finite sum of harmonic oscillators. Also, the crystalline to amorphous transition induced by ion implantation has been experimentally studied and the measured dielectric functions have been fitted by the same set of harmonic oscillators. It has been found that the optical properties of implanted material cannot be modelled using a simple physical mixture of c-GaAs and a-GaAs. Therefore, the HOA appears to be more suitable than the EMA for nondestructive damage depth profiling of shallow implantation. In this case, some artifacts of the EMA can be avoided by the HOA, and the resulting profile agrees well with the profile measured destructively.

This approach is general. Dielectric functions of other semiconductors can also be represented as sums of harmonic oscillators. One possible application is to model the dielectric functions of an alloy (for instance, $Ga_{1-x}Al_xAs$). The resulting dielectric response is then a function of only one parameter: the composition of the alloy (for instance, Al composition).[20] One can also model the variation of the dielectric function with the temperature.[21] This is quite useful, because *in situ* ellipsometry is used on systems which are often not at room temperature. Multilayer analysis is still possible, but one has to know the temperature dependence of the optical properties of all reference materials.

[1]D. E. Aspnes, S. M. Kelso, C. G. Olson, and D. W. Lynch, Phys. Rev. Lett. **48**, 1863 (1982).
[2]M. Erman and J. B. Theeten, Surf. Interface Anal. **4**, 98 (1982).
[3]D. A. G. Bruggeman, Ann. Phys. (Leipzig) **24**, 636 (1936).
[4]H. W. Verleur, J. Opt. Soc. Am. **58**, 1356 (1968).
[5]B. G. Martin and R. F. Wallis, Solid State Commun. **21**, 385 (1977).
[6]V. V. Sobolev, S. A. Alekseeva, and V. L. Gorenberg, Zh. Prikl. Spektrosk. **31**, 675 (1979) [Sov. J. Appl.Spectrosc. **31**, 1274 (1979)].
[7]D. E. Aspnes and A. A. Studna, Appl. Opt. **14**, 220 (1975); Rev. Sci. Instrum. **49**, 291 (1978).
[8]D. E. Aspnes and A. A. Studna, Appl. Phys. Lett. **39**, 316 (1981).
[9]D. E. Aspnes, Am. J. Phys. **50**, 704 (1982).
[10]O. Wiener, Abht. Math. Phys. Kl, Konig. Saechs. Ges. **32** 509 (1912).
[11]D. E. Aspnes, J. B. Theeten, and F. Hottier, Phys. Rev. B **20**, 3292 (1979).
[12]Z. Hashin and S. Shtrikman, J. Appl. Phys. **33**, 3125 (1962).
[13]D. J. Bergman, Phys. Rev. Lett. **44**, 1285 (1980).
[14]D. W. Milton, Appl. Phys. Lett. **37**, 300 (1980).
[15]H. Ehrenreich and M. H. Cohen, Phys. Rev. **115**, 786 (1959).
[16]D. E. Aspnes and A. A. Studna, Phys. Rev. B **27**, 985 (1983).
[17]J. B. Theeten, F. Simondet, M. Erman, and J. Pernas, Proceedings of the 4th International Conference on Solid Surfaces (Cannes, France, Sept. 1980), Le Vide (Les Couches Minces) **201**, 1071 (1980).
[18]J. B. Theeten, D. E. Aspnes, F. Simondet, M. Erman, and P. C. Mürau, J. Appl. Phys. **52**, 6788 (1981).
[19]G. P. Schwartz, B. Schwartz, J. E. Griffits, and T. Sugano, J. Electrochem. Soc. **127**, 2269 (1980).
[20]M. Erman (unpublished).
[21]M. Erman, J. B. Theeten, N. Vodjdani, and Y. Demay, J. Vac. Sci. Technol. **B1**, 328 (1983).